Investigations on vibrational and optical properties of 4-chloro 2-nitroaniline for Nonlinear Optical Applications

K. Sangeetha[1], R. Mathammal[2*], L.Guru Prasad[3]
[1]Department of Physics, Government Arts College, Salem-7
[2]Department of Physics, Sri Sarada College for Women, Salem-16
[3]Department of Science & Humanities, M. Kumarasamy College of Engineering, Karur.
*Corresponding author: E-Mail: Sangeethak2313@gmail.com

ABSTRACT

Quantum mechanical calculations of 4-chloro 2-nitroaniline are carried out by using DFT /B3LYP/6-31+ G (d,p) method. Both the experimental and theoretical vibrational spectrum confirms the presence of functional groups. Electric dipole moment, polarizability and the first order hyperpolarizability values have been computed theoretically. The ^{1}H and ^{13}C nuclear magnetic resonance (NMR) chemical shift of the molecules were calculated by the gauge independent atomic orbital (GIAO) method and compared with experimental results. The calculated HOMO and LUMO energies shows that charge transfer occurs within the molecule. The harmonic vibrational frequencies calculated have been compared with experimental FTIR and FT Raman spectra. The observed and the calculated frequencies are found to be in good agreement.

KEY WORDS: Vibration, optical, quantum.

1. INTRODUCTION

Vibrational assignments based on FT-IR in the vapour, solution, liquid phases and the Raman spectra in the liquid state were reported for aniline**.** The main objective of this paper is to present, more accurate molecular geometry and molecular vibrational assignment of the title molecule. For that purpose quantum chemical computations were carried out on 4Cl2NA using DFT with basis set 6-31G (d,p).The calculated HOMO (Highest occupied molecular orbitals)–LUMO (Lowest unoccupied molecular orbitals) energies show that charge transfer occurs within the title molecule. Density Functional Theory (DFT) calculations have been performed to support our wave number assignments. The theoretically predicted IR and Raman intensities are well in agreement with that of experimental spectral data.

1.1. Computational Details: All calculations were performed using GAUSSIAN program package and the vibrational modes were assigned by means of visual inspection using GAUSSVIEW program and also from the results of normal coordinate calculations. The Cartesian representation of the theoretical force constants have been computed at optimized geometry by assuming C1 point group symmetry, scaling of the force fields were performed by the scaled quantum mechanical procedure. The theoretical results have enabled us to make the detailed assignments of the experimental IR and Raman spectra of the title molecule.

The full molecular geometry optimizations in the ground state was studied by the DFT with the three-parameter hybrid functional (B3) for the exchange part and the Lee–Yang–Parr (LYP) correlation function, using 6-31+G(d, p) basis set. The Cartesian representation of the theoretical force constants are computed at optimized geometry by assuming C1 point group symmetry. An empirical uniform scaling factor of 0.956 was used to offset the systematic errors caused by basis set incompleteness and to neglect the electron correlation and vibrational anharmonicity .The calculated IR and Raman spectra have been found to match well with the experimental spectra. Total energy distribution (TED) calculations, which show the relative contributions of the internal coordinates to each normal vibrational mode of the molecule, and thus enable us to illustrate the character of each mode were carried out by SQM method, using the output files created at the end of the frequency calculations.

1.2. Geometrical structures: The optimized structure of the 4Cl2NA compound is shown in Fig.1. The geometry of the molecules under investigation is considered to possess C1 point group symmetry. The 42 fundamental modes of vibrations of each compound are distributed into the irreducible representation under C1 symmetry as $\Gamma3N{-}6vib{=}$ 42. All vibrations are active in both IR and Raman.

1.3. Vibrational analysis: The present molecule 4Cl2NA consists of 16 atoms, so it has 42 normal vibrational modes. On the basis of C1 symmetry the 42 fundamental vibrations of the title molecule can be distributed as 29A+ 13A. The vibrations of the A species are out-of-plane. All vibrations are active in both IR and Raman. Fig.2. represents the experimental and theoretical FT-IR spectra. The experimental and theoretical Raman spectra are shown in Fig.3. For comparative purposes, the calculated intensity and activity is plotted against the harmonic vibrational frequencies. The resulting vibrational frequencies for the optimized geometries and the proposed vibrational assignments as well as IR intensities and Raman scattering activities are given in Table 2. In the last column is given a detailed description of the normal modes based on the potential energy distribution (PED). The symmetry species of all the vibrations are written in the first column of the table. Modes are numbered from biggest to smallest frequency within each fundamental wave numbers.

1.4. C-H Vibrations: Aromatic compounds commonly shows the presence of C-H stretching vibrations in the region 3000–3100 cm^{-1}. The bands due to C-H in-plane ring bending vibrations, interacting somewhat with C-C stretching vibrations, are observed as a number of medium–weak intensity sharp bands in the region 1300–1000 cm^{-1}. The C-H out-of-plane bending vibrations are strongly coupled vibration and occur in the region 900–667 cm^{-1}. The 4Cl$_2$NA molecule give rise to three C-H stretching, three C-H in-plane bending vibrations and three C-H out-of-plane bending vibrations. In this present work, the FTIR band at 3098, 3075, 3043 cm^{-1} and Raman band at 3095, 3072, 3046 cm^{-1} are assigned to C-H stretching vibrations. The peaks at 1306, 1225, 1128 and 1043 cm^{-1} in FTIR and 1305, 1221 and 1045 cm^{-1} in FT-Raman are assigned to C-H in-plane bending vibrations. The wavenumber of the vibrational bands are shifted to higher values due to steric effect of nitro group. In this title compound, the peaks at 901, 869, and 785 cm^{-1} in FTIR and 898 and 871 cm^{-1} in FT-Raman spectrum confirms the C-H out-of-plane bending vibrations

1.5. C-C vibrations: The carbon–carbon stretching modes of the phenyl group are expected in the range from 1650 to 1200 cm^{-1}. In the present work, the wavenumbers observed in the FTIR spectrum at 1592, 1525, 1490, 1372, 1326 cm^{-1} and in FT-Raman spectrum at 1595, 1527, 1493, 1375, 1323 cm^{-1} have been assigned to C-C stretching vibrations. In the present study, the calculated vibrational wavenumbers are in good agreement with the experimental values. The C-C-C in-plane bending vibrations were observed at 872,838,790,518 cm^{-1} for FTIR spectrum and in FT-Raman spectrum at 892,845,772,550 cm^{-1}. The C-C-C out-of-plane bending vibrations are attributed to the low wavenumbers computed at 567,342,209,147 cm^{-1} for FTIR spectrum and the same was absent in FT-Raman spectrum.

1.6. C-Cl vibrations: The vibrations belonging to the bond between the ring and halogen atoms are worth for the discussion here since the mixing of vibrations are possible due to the lowering of the molecular symmetry and the presence of heavy atoms on the periphery of molecule. Generally C-Cl absorption was obtained in the region 850–550 cm^{-1}. Therefore the peaks identified at 707 cm^{-1} in the FTIR spectrum and 710 cm^{-1} in the FT-Raman spectrum had been assigned to C-Cl stretching mode vibrations of 4Cl2NA respectively. Most of the aromatic chloro compounds have the strong to medium intensity in the region 385-265 cm^{-1} due to C-Cl in-plane bending vibration. The IR band identified at 352cm^{-1} are assigned to the C-Cl in plane bending vibration, 180 cm^{-1} are assigned to the C-Cl out-of- plane deformation vibration of the title compound.

1.7. NO$_2$Vibration: Aromatic nitro compounds have strong absorptions due to asymmetric and symmetric stretching vibrations of the nitro group at 1570–1485 and 1370–1320 cm^{-1}. This could be due to the electron withdrawing substituent adjacent to the nitro group which tend to increase the frequency of asymmetric vibration and decrease that of the symmetric vibration. In the present work, the bands observed at 1525 cm^{-1} in the FTIR and 1527 cm^{-1} in the FT-Raman spectrum are assigned to asymmetric stretching vibrations. The title molecule shows band at 1372 cm^{-1} in the FTIR and 1375 cm^{-1} in the FT-Raman spectrum and are assigned to symmetric stretching vibration. The deformation vibrations of NO$_2$ group (rocking, wagging and twisting) contribute to several normal modes in the low frequency region. These bands are also found in the wavenumber region around the characteristic position 862 cm^{-1} in FTIR and 860 cm^{-1} in FT-Raman spectrum for 4Cl2NA. The NO$_2$ torsion vibration is observed in the Raman spectrum at 60 cm^{-1}.

1.8. NH$_2$ Vibration: In all the primary aromatic amines, the N-H stretching frequencies occur in the region 3300-3500 cm^{-1}. The title molecule under investigation possesses one NH$_2$ group and hence we expect one symmetric and one asymmetric N-H stretching vibrations. . In the present molecule, the band which is observed at 3564 cm^{-1} in the FT-IR and 3560 cm^{-1} in the FT-Raman spectrum are assigned to asymmetric stretching vibration. In the present molecule, the band at 3564 cm^{-1} and 3560 cm^{-1} which is assigned to asymmetric stretching vibration are shifted to higher values due to intermolecular hydrogen bonding and inductive effect. Symmetric stretching vibration of NH$_2$ group band is observed at 3420 cm^{-1} in the FT-IR and counter part of FT-Raman spectrum shows at 3417 cm^{-1}. The NH$_2$ group also has scissoring (δ NH$_2$) rocking (ρNH$_2$), wagging (ωNH$_2$) and torsion (τNH$_2$) modes. The scissoring mode of the NH$_2$ group appears in the region1615-1650 cm^{-1} in benzene derivatives with NH$_2$ substituents. The computed NH$_2$ scissoring vibration shows bands with FT-IR at 1546 cm^{-1} and FT-Raman at 1543 cm^{-1}. In the present molecule, the band at 1546 cm^{-1} and 1543 cm^{-1} which is assigned to scissoring vibration are shifted to lower values due to intermolecular hydrogen bonding. The NH$_2$ rocking mode shows recorded FT-IR band at 987 cm^{-1} and FT-Raman at 983 cm^{-1}. The NH$_2$ wagging mode shows recorded FT-IR at 389 cm^{-1} and FT-Raman at 385 cm^{-1}. The NH$_2$ torsion vibration was observed in the FT-IR at 201 cm^{-1} and the same was absent in FT-Raman spectrum.

1.9. NMR analysis: DFT methods treat the electronic energy as a function of the electron density of all electrons simultaneously and thus include electron correlation effect. The ^{13}C and ^{1}H theoretical and experimental chemical shifts of the title molecule are tabulated in Table.1. In this study, molecular structure of the 4Cl$_2$NA was optimized by using B3LYP method in conjunction with 6-31G∗. 13C and 1H chemical shift calculations of the title compounds have been made by using GIAO method and same basis set. The B3LYP method allows calculating the shielding constants with the proper accuracy, and the GIAO method is one of the most common approaches for calculating

nuclear magnetic shielding tensors. The experimental and calculated NMR spectra of 4Cl2NA are shown in Figs. 4-5.

The approximate chemical shift ranges of some 13C resonances i.e., C of aromatic ring have the δ range 110–160 and type of carbon having double bond oxygen is in the δ range 150–220. In our title compound, the nitrogen atom is in the para position. This nitrogen atom shows electronegative property. The oxygen atom of nitro group is electron withdrawing group, so deshielding occurs and chemical shift of C1 and C5 is high. The other carbon atoms of the benzene structure gives the chemical shift at 129.97, 123.96, 121.10 and 118.33 ppm.

The aromatic protons are having the chemical shift δ (ppm) in the range 6–8.5 [13]. The signals at **δ=8.608 ppm** is due to aromatic protons. Here there is more deshielding and hence the chemical shift increases. The signals at 8.608, 8.454, 7.490 and 6.85 ppm are due to the presence of hydrogen atom in the aromatic ring. Here there is more deshielding due to electronegative oxygen atoms and hence the chemical shift increases. And the signal at 8.454 ppm and 4.712 ppm is due to proton of the amine group. As the hydrogen atom is surrounded by electronegative oxygen atoms, there will be more shielding around it and hence the chemical shift falls at up field with low ppm value. Since, greater the degree of hydrogen bonding of a proton, greater is the downfield shift.

1.10. NLO analysis: The values of the polarizability tensor components for a given system will depend on the choice of the Cartesian co-ordinate system used. The molecule for which $\alpha_{xx} = \alpha_{yy} = \alpha_{zz}$ is said to be isotropic. The polarizability is isotropic or is the same in all directions for a molecule whose electron density is spherically symmetrical. If the molecules are perfectly isotropic (p) and (E) will have the same direction and is then a simple scalar quantity. If the molecule is anisotropic, $\alpha_{xx} \neq \alpha_{yy} \neq \alpha_{zz}$ (p) will no longer have the same direction as (E). The intensity of Raman scattering may be proportional to the derived polarizability components. To express the scattering intensity in terms of the derived polarizability tensor, the quantities ($\bar{\alpha}$) and the anisotropy invariant (γ) are necessary. They are constant regardless of the orientation of the molecules. The quantity ($\bar{\alpha}$) is the mean value of the three principle components of ($\bar{\alpha}$) and (γ) measures the anisotropy of the tensor. The polarizability, the first hyperpolarizability and the anisotropy polarizability invariant are computed with the numerical derivative of the dipole moment using B3LYP/6-31+G (d,p) are presented in Table 2. The definitions for the isotropic polarizability is

$\bar{\alpha} = 1/3(\alpha_{xx} + \alpha_{yy} + \alpha_{zz})$

Using the x, y and z components the magnitude of the total static dipole moment (μ), isotropic polarizability (α_0), first-order hyperpolarizability (β_{total}) tensor, can be calculated by the following equations:

$\mu^0 = (\mu_x^2 + \mu_y^2 + \mu_z^2)^{1/2}$

$\beta_{tot} = (\beta_x + \beta_y + \beta_z)^{1/2}$

The complete equation for calculating the first-order hyperpolarizability from GAUSSIAN 09W output is given as follows: $\beta_{tot} = [(\beta_{xxx} + \beta_{xyy} + \beta_{xzz})^2 + (\beta_{yyy} + \beta_{yzz} + \beta_{yxx})^2 + (\beta_{zzz} + \beta_{zxx} + \beta_{zyy})^2]^{1/2}$.

The β components of GAUSSIAN 09 W output are reported in atomic units, the calculated values have to be converted into electrostatic units (1 a.u. = 8.3693X 10^{-33} esu).

The polarizabilities and hyperpolarizabilities characterize the response of a system in an applied electric field. Theoretical calculation provides another method to investigate substantial characteristics of materials. The first order hyperpolarizability (β) of the title molecule is calculated using B3LYP 6-31+G (d,p) basis set based on the finite field approach. Hyperpolarizability is a third rank tensor that can be described by a 3×3×3 matrix. The calculated first-order hyperpolarizability (β_{tot}) value of 4Cl2NA is 1.11064 x10^{-30} esu, which is nearly 6 times greater than that of urea (0.1947x10^{-30} esu). The large β value calculated by B3LYP method reveal that the title molecule can be used as a good candidate for frequency conversion application. The theoretical calculation of β components is very useful as it clearly indicates the direction of charge delocalization. The large β value calculated by B3LYP method reveal that the title molecule can be used as a good candidate for frequency conversion application.

1.11. HOMO-LUMO analysis: Many organic molecules that contain conjugated π electrons are characterized as hyperpolarizabilities and were analysed by means of vibrational spectroscopy. In most of the cases, even in the absence of inversion symmetry, the strongest band in the Raman spectrum are weak in the IR spectrum and vice-versa. The π electron cloud moment from the donor to acceptor can make the molecule highly polarized through the single –double path when it changes from the ground state to the first excited state. The HOMO, LUMO and HOMO-LUMO energy gap of 4Cl2NA in DFT level in 6-31 G (d,p) basis set has been calculated. The HOMO–LUMO energy gap reveals that the energy gap reflects the chemical activity of the molecule.

HOMO energy = −0.23914 a.u.

LUMO energy = −0.10698 a.u.

HOMO–LUMO energy gap = -0.1321 a.u.

Electronegativity (χ)　　　　$\mu = -\chi = \dfrac{-IP + EA}{2}$

Chemical hardness　　　　$\eta = \dfrac{IP - EA}{2}$

Softness $\zeta = 1/2\ \eta$
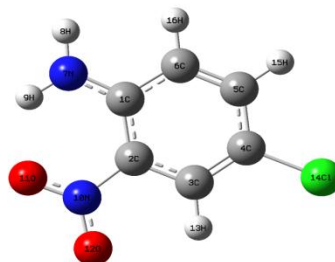Electrophilicity index $\psi = \mu^2/2\ \eta$

The calculated self-consistent field (SCF) energy of 4Cl2NA is -951.737351537 a.u. The values of electronegativity, hardness (η), softness (ζ) and electrophilicity index (ψ) that are obtained for title molecule as -0.34612, 0.13216, 3.783292 and 0.45323 respectively. The HOMO and LUMO diagram of 4Cl2NA are shown in Fig. 6-7. Moreover, lowering in the HOMO and LUMO energy gap explains the eventual charge transfer interactions that take place within the molecule.

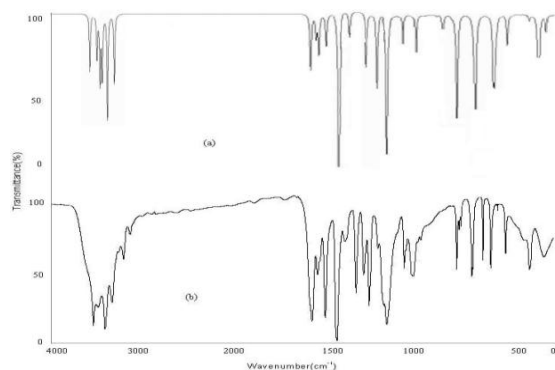**Table.1.Experimental and calculated ^{13}C NMR and ^{1}H NMR Chemical shifts (ppm) of 4Cl2NA**

	Experimental	B3LYP/6-31G+ (d,p)
C_1	145.03	130.15
C_5	135.47	122.58
C_2	129.97	119.58
C_4	123.96	117.11
C_3	121.10	115.02
C_6	118.33	104.53
H_{13}	7.891	8.608
H_9	7.543	8.454
H_{15}	7.384	7.490
H_{16}	7.364	6.85
H_8	7.041	4.712
H	7.020	-

Table.2.Polarizability and hyperpolarizability values of 4C2NA

Parameters	B3LYP / 6-31G(d,p)
α_{xx}	130.0733
α_{xy}	-5.575286
α_{yy}	153.196473
α_{xz}	0.0339219
α_{yz}	-0.0636108
α_{zz}	56.150543
α_{tot}	**1.67673×10^{-23}e.s.u**
β_{xxx}	-64.5112199
β_{xxy}	50.51130
β_{xyy}	233.229051
β_{yyy}	56.277709
β_{xxz}	0.0051631
β_{xyz}	-0.0629148
β_{yyz}	0.0759128
β_{xzz}	0.841528
β_{yzz}	-2.38644
β_{zzz}	-0.0031338
β_{tot}	**1.66653×10^{-30}e.s.u**

Figure.1. Molecular Structure of 4Cl2NA

Fig.2.Observed and calculated FT-IR spectra of 4Cl2NA

Fig.3.Observed and calculated FT-Raman spectra of 4Cl2NA

Fig 4(a): Theoretical ^{13}C NMR Spectrum

Fig 4(b): Experimental ^{13}C NMR Spectrum

Fig 5(a): Theoretical ^{1}H NMR Spectrum

Fig 5(b): Experimental ^{1}H NMR

Fig.6. HOMO = -0.23914

Fig.7. LUMO = -0.10698

2. CONCLUSION

The vibrational properties of DBSA have been investigated by FT-IR and FT-Raman spectroscopies and were performed on the basis of DFT/B3LYP/6-31+G (d,p) basis set level. A comparison of the result of experimental and theoretical study gave us a full description of the geometry and vibrational properties of the compound. The calculated HOMO and LUMO energies shows that charge transfer occurs within the molecule. ^{1}H and ^{13}C NMR chemical shifts are compared with experimental values. The electric dipole moment, polarizability and the first order hyperpolarizability of the title compound were calculated. The ^{13}C chemical shifts of all the carbon atoms and ^{1}H NMR chemical shifts of all the aromatic protons are in good agreement with the experimental values.

3. ACKNOWLEDGEMENTS

REFERENCES

Arivazhagan M, Jeyavijayan S, FTIR and FT-Raman spectra, assignments, ab initio HF and DFT analysis of xanthine, Spectrochim. Acta A, 79, 2011, 161-168.

Arjunan V, Mohan S, Fourier transform infrared and FT-Raman spectral analysis and ab initio calculations for 4-chloro-2-methylaniline and 4-chloro-3-methylaniline, J.Mol.Struct., 892, 2008, 289-299.

Avci D, Atalay Y, Sekerci M, and Dincer M, Molecular structure and vibrational and chemical shift assignments of 3-(2-Hydroxyphenyl)-4-phenyl-1H-1,2,4-triazole-5-(4H)-thione by DFT and ab initio HF calculations, Spectrochimica Acta A,73 (1), 2009, 212–217.

Evans J.C, The vibrational assignments and configuration of aniline, aniline-NHD and aniline-ND$_2$, Spectrochim Acta., 16, 1960, 428-442.

Gunasekaran S, Balaji R.A, Kumeresan S, Anand G, Srinivasan S, Can, Experimental and theoretical investigations of spectroscopic properties of N-acetyl-5-methoxytryptamine, J.Anal.Sci.Spectrosc., 53, 2008, 149–162.

Karabacak M, Kurt M, The spectroscopic (FT-IR and FT-Raman) and theoretical studies of 5-bromo-salicylic acid, J. Mol. Struct., 919, 2009, 215–222.

Krishnakumar V, and Mathammal R, Density functional and experimental studies on the FT-IR and FT-Raman spectra and structure of benzoic acid and 3, 5-Dichloro Salicylic acid, Journal of Raman Spectroscopy, 40 (3), 2009, 264-271.

Krishnakumar V, Nagalakshmi R, Studies on the first-order hyper polarizability and terahertz generation in 3-nitroaniline, Physica B, 403, 2008, 1863–1869.

Lee C, Yang W, and Parr R.G, Development of the Colle-Salvetti correlation-energy formula into a functional of the electron density, Phys. Rev.B., 37, 1998, 785-789.

Pulay P, Fogarasi G, Pongor G, Boggs J.E, Vargha A, Combination of theoretical ab initio and experimental information to obtain reliable harmonic force constants. Scaled quantum mechanical (QM) force fields for glyoxal, acrolein, butadiene, formaldehyde, and ethylene, J. Am. Chem. Soc., 105, 1983, 7037-7047.

Sathyanarayana D.N, Vibrational Spectroscopy—Theory and Applications, New Age International Publishers, New Delhi, 2004.

Silverstein M, Clayton Basseler G, Morill C, Spectrometric Identification of Organic Compounds, Wiley, New York, 1981.

Silverstein M, Clayton Basseler G, Morill C, Spectrometric Identification of Organic Compounds, Wiley, New York, 1981.

Vijayakumar T, Hubert Joe I, Nair C.P.R, and Jayakumar V.S, Efficient π electrons delocalization in prospective push–pull non-linear optical chromophore 4-[*N,N*-dimethylamino]-4′-nitro stilbene (DANS): A vibrational spectroscopic study, Chem.phys., 343, 2008, 83-99.

Yadav L.D.S, Organic Spectroscopy, second ed., Anamaya Publishers, New Delhi, 2007.

Yadav R.A, and Singh I.S, Intermolecular hydrogen-bonding in o-ethyl and m-ethyl phenols, Ind.J. Pure Appl.Phys., 23, 1985, 626.